Hindawi Publishing Corporation
Research Letters in Physical Chemistry
Volume 2008, Article ID 346545, 4 pages
doi:10.1155/2008/346545

Research Letter

Hydriding Reaction of $LaNi_5$: Correlations between Thermodynamic States and Sorption Kinetics during Activation

P. Millet,[1] C. Lebouin,[2] R. Ngameni,[1] A. Ranjbari,[1] and M. Guymont[1]

[1] *Institut de Chimie Moléculaire et des Matériaux, CNRS UMR 8182, Université Paris Sud, 15 rue Georges Clémenceau, 91405 Orsay Cedex, France*
[2] *Laboratoire d'Electrochimie et de Physicochimie des Matériaux et des Interfaces, CNRS UMR 5631-INPG-UJF, ENSEEG, 1130 rue de la piscine, 38402 Saint Martin d'Hères, France*

Correspondence should be addressed to P. Millet, pierre.millet@u-psud.fr

Received 25 October 2007; Accepted 11 March 2008

Recommended by Vasudevanpillai Biju

This research work concerns the hydriding reaction of $LaNi_5$ during the first hydriding cycles (activation process). Step-by-step sorption isotherms (Δ[H/M] $\approx$ 0.03) were measured at 298 K, in the composition range 0 < H/M < 2.0, at the beginning (first hydriding cycle, where hysteresis is maximum) and at the end (tenth hydriding cycle, where hysteresis is minimum) of the activation process, offering the possibility to correlate thermodynamic states (pressure-composition data points) to sorption kinetics. Using pneumatochemical impedance spectroscopy (PIS), experimental impedance diagrams were obtained for each data point of the isotherms. Microscopic rate parameters such as surface resistance and hydrogen diffusion coefficient were obtained as a function of composition, by fitting appropriate model equations to experimental impedances. It is found that the high-frequency pneumatochemical resistance significantly decreases during activation. This is correlated with the surface increase of the solid-gas interface area. The hydrogen diffusion coefficient is found to be larger at the beginning of the activation process and lower on a fully activated sample.

1. INTRODUCTION

Metal-hydride systems are increasingly studied for hydrogen-storage applications. In particular, many intermetallic compounds (IMCs) such as the Haucke (AB_5) phases offer several interesting features, in terms of specific energy, volumetric energy, and kinetics. Practical applications require the determination of both thermodynamic and kinetic properties which are, in general, measured separately. Pneumatochemical impedance spectroscopy (PIS) [1] now offers the possibility of analyzing hydriding/dehydriding reaction mechanisms, raw kinetic data being measured using a classical Sieverts experimental setup [2]. Using PIS, kinetic information is not only a measure of a global reaction rate (limited by any rate-determining step): the different steps involved in the sorption reaction are put into evidence and the values of individual rate parameters are inferred. Results obtained so far on various IMCs indicate that most hydriding mechanisms involve two microscopic reaction steps: (i) the surface chemisorption of molecular hydrogen which is dissociated into two surface ad-atoms; (ii) the diffusion-controlled transport of hydrogen atoms to bulk regions where they can either accumulate (in solid-solution domains) or precipitate to form metal hydrides (in two-phase domains). PIS is therefore an in situ spectroscopic tool which can be used to analyze surface and bulk processes in solid-gas systems.

Activation is the term referring to the first hydriding cycles of a brittle hydrogen absorbing IMC, during which the sample is gradually pulverized into a powder of fine particles. This pulverization is induced by the precipitation of a hydride phase of larger lattice parameters than the host IMC. This in turn generates internal strain and stresses and leads to the formation of a few micrometers thick particles, with large concentration of defects. During activation, thermodynamic properties (in particular pressure-composition equilibrium isotherms) and sorption kinetics are significantly modified. Whereas it is known from the literature that the absorption

pressure plateau significantly decreases during the first hydriding cycles [3]; it is still unclear how individual rate parameters (surface resistance and hydrogen diffusion coefficient) are related to the thermodynamic states of the sample. The purpose of the work presented here is therefore to correlate thermodynamic states and sorption kinetics measured during the activation of $LaNi_5$.

2. EXPERIMENTAL SECTION

The basic principles and details about pneumatochemical impedance spectroscopy have been previously reported [1]. A thorough description of the experimental setup and experimental requirements for measuring pneumatochemical impedances is described in [4]. In the present work, 2.9 g of $LaNi_5$ powder (Alfa Aesar GmbH, Karlsruhe, Germany) were placed in the reaction chamber of the PIS setup. Because the sample is prone to surface oxidation [5], it was loaded in an inert atmosphere of argon using a glove box. The setup can be gas-purged down to secondary vacuum levels (1×10^{-6} mbar) using a turbomolecular pumping station (BOC Edwards Co., Crawley, UK) to remove any residual impurity. Alphagaz grade 1 H_2 (Air Liquide Co., Paris, France) was used in the experiments.

3. RESULTS AND DISCUSSION

3.1. Experimental results

Two pressure-composition isotherms, measured at 298 K on $LaNi_5$-H_2 (g) up to the composition point H/M ≈ 2, are plotted in Figure 1(a) (the maximum composition at 298 K, not represented here, is H/M ≈ 5.8). The first isotherm was recorded during the first hydriding cycle and the second one was recorded at the end of the activation process, during the 10th hydriding cycle. At low-hydrogen content (0.0 < H/M < 0.5), a solid solution of hydrogen (α-$LaNi_5$) is formed. As the hydrogen content increases, a nonstoechiometric hydride phase ($LaNi_5H_{6-x}$ or β-$LaNi_5$ phase) begins to be formed. The system becomes monovariant and a pressure plateau develops. This is the two-phase domain which extends over the 0.5 < H/M < 5.8 composition range. At higher hydrogen contents, a solid solution of hydrogen in β-$LaNi_5$ is formed. In this research work, experiments plotted in Figure 1 were intentionally stopped at H/M ≈ 2.0 to avoid lengthy and unnecessary measurements over the whole composition range.

The main characteristic associated with metal-hydride systems is the presence of a large hysteresis. The difference between absorption and desorption plateau pressures is significantly large (*ca.* 1400 mbar) for the first isotherm (Figure 1(a)). The amplitude of hysteresis decreases during activation, and a final value of *ca.* 400 mbar, observed during the 10th hydriding cycle (Figure 1(a)), is typical of an activated material. Hysteresis also exists at phase boundaries, the composition at which the first hydride nucleus is formed during absorption being different from the composition at which the last hydride nucleus disappears during desorption (Figure 1(a)).

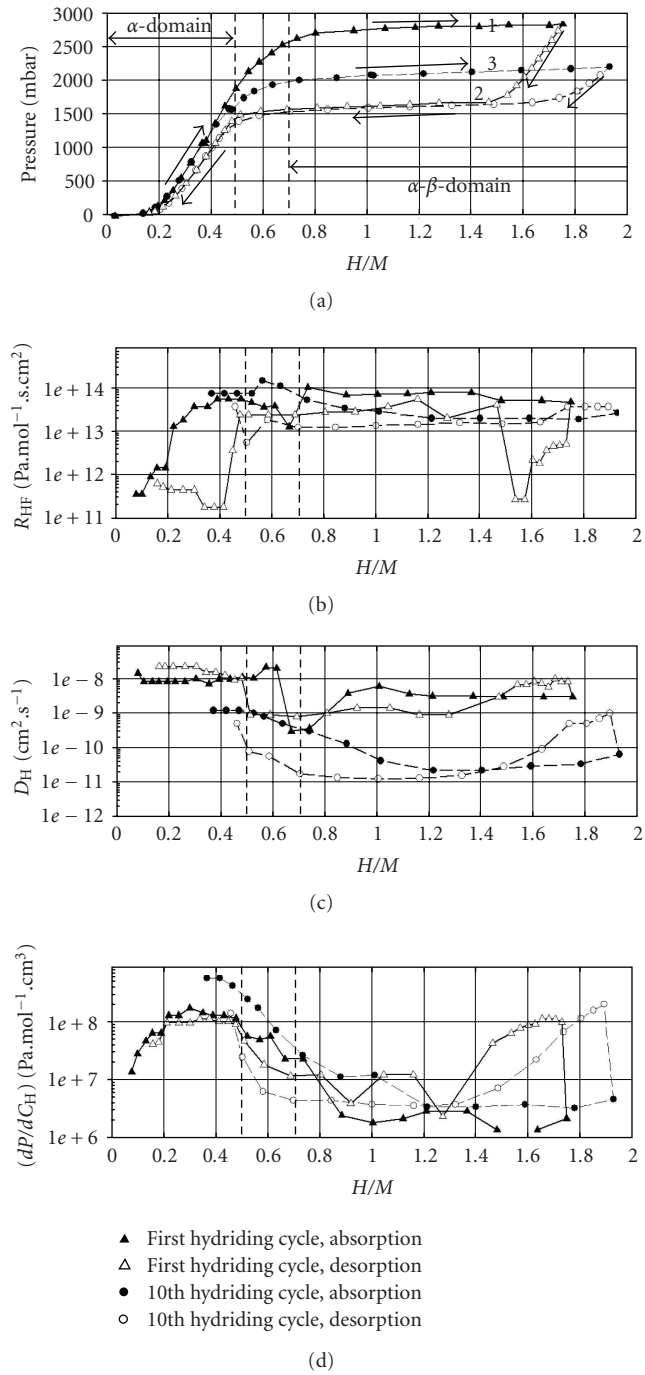

FIGURE 1: (a) Equilibrium pressure; (b) R_{HF}; (c) D_H; (d) dP/dC_H as a function of composition H/M measured on $LaNi_5$ at 298 K. (Data points labelled 1, 2, 3 in (a) refer to the impedance diagrams of Figure 2.)

Each data point of Figure 1(a) corresponds to one gas transfer experiment during which the transient pressure measured in the reaction chamber and the transient hydrogen mass flow entering the reaction chamber were synchronously sampled, yielding one impedance diagram per experiment. Typical impedance diagrams measured during activation in two-phase domains are plotted in Figure 2.

Impedance spectra numbers (1, 2, 3) of Figure 2 are referring to the gas transfer experiments (1, 2, 3) of Figure 1(a). They are expressed in $\mathrm{Pa \cdot mol^{-1} \cdot s}$ and not in $\mathrm{Pa \cdot mol^{-1} \cdot s \cdot cm^2}$, that is, they are not corrected for the solid-gas interface area. As analyzed elsewhere [1], in two-phase domains, a typical semicircle is observed in the high-frequency (HF) domain along the real axis (see, e.g., diagram 1 in Figure 2). This is the signature of the parallel connection of a capacitance (associated with the dead volume of the reaction chamber) and a resistance in $\mathrm{Pa \cdot mol^{-1} \cdot s}$. In single-phase domains (SPDs), the diameter of this HF semicircle is equal to the value of the surface resistance R_s (the chemisorption step of the sorption process) but in two-phase domains (TPDs), this is the sum ($R_s + R_{PT}$), R_{PT} being the resistance associated with the phase transformation process [6]. The HF semicircle is then followed at lower frequencies by a characteristic medium frequency (MF) region related to hydrogen diffusion and ends up at low frequencies (LF) in a capacitive shape (a semi-infinite line along the imaginary axis).

Each experimental impedance diagram of Figure 1(a) was fitted using model equations applicable to single- and two-phase domains, as described in [6]. From the fits, values of the HF resistance (R_{HF}), the hydrogen diffusion coefficient (D_H), and the slope of the isotherm at the measurement point (dP/dC_H) were obtained. All results are plotted as a function of the composition H/M in Figures 1(b), 1(c), and 1(d), respectively. In Figure 1(b), the true solid-gas interface area has been taken into account and R_{HF} values are expressed in $\mathrm{Pa \cdot mol^{-1} \cdot s \cdot cm^2}$.

3.2. Shape of impedance diagrams during activation

The first impedance diagram of Figure 2 (curve 1) was measured on the unactivated sample, on the pressure plateau in the two-phase domain (data point 1 in Figure 1(a)). A large HF resistance of *ca.* 4×10^{11} $\mathrm{Pa \cdot mol^{-1} \cdot s}$ is observed. Once the scan is reversed, the first impedance diagram measured on the desorption pressure plateau (point 2 in Figure 1(a)) is also plotted in Figure 2 (curve 2). An overall lower HF resistance is measured but two consecutive semicircles are observed, suggesting a bimodal distribution of particle size. In other experiments (not reported here), more than two HF semicircles were observed. It can be concluded that fragmentation of initial particles leads to particles of heterogeneous sizes. Finally, the impedance diagram measured in two-phase domains on the activated sample (point 3 in Figure 1(a)) is also plotted in Figure 2 (curve 3). The impedance is significantly lower for each frequency, indicating that the sorption kinetics will be higher on the activated sample.

3.3. High-frequency resistance

It is observed from the whole set of experimental impedance diagrams (not represented here) that the high-frequency resistance R_{HF} (expressed in $\mathrm{Pa \cdot mol^{-1} \cdot s}$) decreases exponentially with the number of hydriding cycles, down to a constant value at the end of the activation process. This does not mean that the kinetics of the surface step (in SPDs) or the phase transformation process (in TPDs) are varying during activation: mostly HF resistances are a function of the operating temperature which is constant here. The reduction of R_{HF} must be correlated with the increasing solid-gas (and interphase) interface areas resulting from the sample pulverization. To take into account the modification of the solid-gas interface area during activation, R_{HF} values plotted in Figure 1(b) are expressed in $\mathrm{Pa \cdot mol^{-1} \cdot s \cdot cm^2}$. Real surfaces areas were estimated from mean particle size values obtained from microscope observations. Assuming that particles are spherical, taking a mean particle radius of 50 μm for the first hydriding cycle and a density of 8.2 for $LaNi_5$ [7], a total surface of 212 $\mathrm{cm^2}$ was used. Taking a mean particle radius of 5 μm for the tenth hydriding cycle, a total surface of 2120 $\mathrm{cm^2}$ was used. When HF resistances are expressed per $\mathrm{cm^2}$ of solid-gas interface, they are mostly constant in TPDs (Figure 1(b)), although their values spread over a decade of units (this comes from experimental uncertainties and the estimation of the true interface area). In SPDs, HF resistances are lower than those in TPDs where R_{PT} values (the resistance associated with the phase transformation process) are included, as discussed in [6]. From the data of Figure 1(b), R_{PT} is found to remain almost constant during activation.

From these results, a limitation of PIS analysis should be pointed out (especially when powdered samples are used, as $LaNi_5$ considered here): the mean particle radius (at the measurement point) must be known to normalize impedance diagrams. This is because different triplet values $\{r; D; dP/dC\}$ lead to similar impedance diagrams. If not, it is difficult to analyze quantitatively the hydriding kinetics.

3.4. Hydrogen diffusion coefficient

Concerning hydrogen diffusion coefficients, the most striking result is that values are spread over several (three) decades of values. General trends are that values measured on unactivated samples are larger than those measured on fully activated samples and that values measured in solid-solution domains are larger than those measured in two-phase domains. At 298 K, D_H values measured on an unactivated sample are within the range 1×10^{-9}–1×10^{-8} $\mathrm{cm^2 \cdot s^{-1}}$, whereas those measured on an activated sample are spread over the 1×10^{-11}–1×10^{-10} $\mathrm{cm^2 \cdot s^{-1}}$ range. It is concluded that large concentrations of defects (point defects, dislocations), appearing in activated samples because of the precipitation of the β-$LaNi_5H$ hydride phase, contribute to a reduction of the kinetics of the diffusion step but a relationship between kinetics and microstructure still needs to be established to clarify the point. Anyway, concerning the overall kinetics, this effect is largely counterbalanced by the large increase of the solid-gas interface area.

3.5. Slope of the isotherm

The slopes of the isotherms obtained from the automated fitting procedure are plotted in Figure 1(d) as a function of hydrogen composition. Although a certain discrepancy is

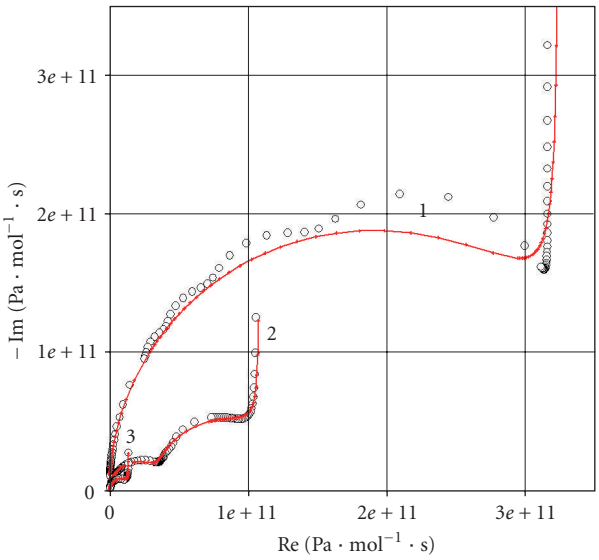

FIGURE 2: Experimental (o) and model (–) impedance diagrams. 1, 2, 3 refer to data points of Figure 1(a). (1) First hydriding cycle, absorption, H/M ≈ 1.5, (2) First hydriding cycle, desorption, H/M ≈ 1.4, (3) 10th hydriding cycle, absorption, H/M ≈ 1.5.

observed, there is a qualitative agreement with the experimental isotherms of Figure 1(a), the slope being larger in solid-solution domains than in two-phase domains, except at the foot of the isotherms where hydrogen trapping effects prevail. From a quantitative viewpoint, care must be taken when comparing the data of Figure 1(d) to the isotherms of Figure 1(a). This is because in Figure 1(a), the hydrogen content is expressed in H/M units whereas in Figure 1(d), the hydrogen content is expressed in concentration (C_H in mol · cm^{-3}).

4. CONCLUSIONS

The hydriding reaction of $LaNi_5$ has been analyzed during the activation process using pneumatochemical impedance spectroscopy. Experimental impedance diagrams have been measured during the first and the tenth hydriding cycle. Using model equations, individual rate parameters (surface resistance and hydrogen diffusion coefficient) have been obtained as a function of composition H/M. Impedance diagrams show that the overall absorption kinetics largely increases during activation. This is mostly due to the increase of the solid-gas interface areas. When the solid-gas surface area is taken into account, it is shown that the high-frequency resistance related to surface hydrogen chemisorption and hydride precipitation remains mostly constant. To a lesser extent, the hydrogen diffusion coefficient decreases during activation. This is attributed to the formation of defects. Results obtained along hysteresis loops will be presented in a subsequent communication.

ACKNOWLEDGMENTS

Financial support from the French Agence Nationale de la Recherche, within the frame of the Plan d'Action National sur l'Hydrogène, EolHy Project (ANR-06-PANH—008-06), is acknowledged.

REFERENCES

[1] P. Millet, "Pneumato-chemical impedance spectroscopy. 1. Principles," *Journal of Physical Chemistry B*, vol. 109, no. 50, pp. 24016–24024, 2005.

[2] A. Sieverts, "Die Aufnahme von Gasen durch Metalle," *Zeitschrift für Metallkunde*, vol. 21, pp. 37–46, 1929.

[3] T. Yamamoto, H. Inui, and M. Yamaguchi, "Effects of lattice defects on hydrogen absorption-desorption pressures in $LaNi_5$," *Materials Science and Engineering A*, vol. 329–331, pp. 367–371, 2002.

[4] P. Millet, C. Decaux, R. Ngameni, and M. Guymont, "Experimental requirements for measuring pneumato-chemical impedances," *Review of Scientific Instruments*, vol. 78, no. 12, Article ID 123902, 11 pages, 2007.

[5] P. Millet, "Pneumato-chemical impedance spectroscopy. 2. Dynamics of hydrogen sorption by metals," *Journal of Physical Chemistry B*, vol. 109, no. 50, pp. 24025–24030, 2005.

[6] P. Millet, C. Decaux, R. Ngameni, and M. Guymont, "Fourier-domain analysis of hydriding kinetics using pneumato-chemical impedance spectroscopy," *Research Letter in Physical Chemistry*, vol. 2007, Article ID 96251, 5 pages, 2007.

[7] J.-M. Joubert, R. Černý, M. Latroche, et al., "A structural study of the homogeneity domain of $LaNi_5$," *Journal of Solid State Chemistry*, vol. 166, no. 1, pp. 1–6, 2002.